

Published in final edited form as:

Carbon N Y. 2016 April ; 99: 229–237. doi:10.1016/j.carbon.2015.12.024.

Retention of ¹⁴C-labeled multiwall carbon nanotubes by humic acid and polymers: Roles of macromolecule properties

Qing Zhao^{a,b,f}, Elijah J. Petersen^{c,*}, Geert Cornelis^d, Xilong Wang^e, Xiaoying Guo^e, Shu Tao^e, and Baoshan Xing^{b,*}

^a Institute of Applied Ecology, Chinese Academy of Sciences, Shenyang 110016, China

^b Stockbridge School of Agriculture, University of Massachusetts, Amherst, MA 01003, USA

^c Biosystems and Biomaterials Division, National Institute of Standards and Technology, Gaithersburg, Maryland 20899, USA

^d Department of chemistry and Molecular Biology, University of Gothenburg, Gothenburg 41296, Sweden

^e Laboratory for Earth Surface Processes, College of Urban and Environmental Sciences, Peking University, Beijing 100871, China

^f Key Laboratory of Pollution Ecology and Environmental Engineering, Institute of Applied Ecology, Chinese Academy of Sciences, Shenyang 110016, China

Abstract

Developing methods to measure interactions of carbon nanotubes (CNTs) with soils and sediments and understanding the impact of soil and sediment properties on CNT deposition are essential for assessing CNT environmental risks. In this study, we utilized functionalized carbon-14 labeled nanotubes to systematically investigate retention of multiwall CNTs (MWCNTs) by 3 humic acids, 3 natural biopolymers, and 10 model solid-phase polymers, collectively termed macromolecules. Surface properties, rather than bulk properties of macromolecules, greatly influenced MWCNT retention. As shown via multiple linear regression analysis and path analysis, aromaticity and surface polarity were the two most positive factors for retention, suggesting retention was regulated by π - π stacking and hydrogen bonding interactions. Moreover, MWCNT deposition was irreversible. These observations may explain the high retention of MWCNT in natural soils. Moreover, our findings on the relative contribution of each macromolecule property on CNT retention provide information on macromolecule selection for removal of MWCNTs from wastewater and provide a method for measuring CNT interactions with organic macromolecules.

* Corresponding author. Tel: 413 545-5212. bx@umass.edu (Baoshan Xing); Tel: 301-975-8142. Elijah.petersen@nist.gov (Elijah J. Petersen).

Appendix A. Supplementary data
Supplementary data associated with this article can be found in the online version.

1. Introduction

Carbon nanotubes (CNTs) are potentially useful in many applications such as electronics, optics, and other fields of material science. During their production, transport, handling, use and disposal, they will inevitably enter the environment. Studies on the toxicity of CNTs showed that under certain conditions, especially those involving chronic exposure, CNTs may pose a risk to human health and organisms in the environment if present at sufficiently high concentrations [1-4]. Therefore, it is essential to know the fate of CNTs once they are released to the environment.

Environmental modeling so far indicates that soils and sediments will be the environmental compartments with the highest CNT concentrations especially if activated sludge, which efficiently removes many nanoparticles, is applied on soils [5-7]. Transport and bioavailability of CNTs in soils depends on the different interactions between CNTs and the soil solid phases such as reversible/irreversible deposition and redispersion, here collectively referred to here as retention [8]. Thus, developing methods to assess retention of CNTs by soils and sediments can help us to better assess their environmental risks in terms of bioavailability to organisms and possible transport to ground water tables. Due to the challenges related to quantification of CNTs in solid samples, studies on CNT retention by soils are limited [9, 10]. In addition, it is not sufficient to only study whole soil samples, because soil is a mixture of mineral and organic constituents. Research on interactions between different constituents of soil and CNTs is necessary to understand the retention mechanisms. Sorption of organic compounds on different fractions of soil organic matter (SOM) has been extensively studied, because of the critical role of SOM in organic compounds' environmental behaviors [11-15]. CNT is a carbon-based material and therefore possibly possesses similar properties compared to organic compounds, but CNTs are also nanomaterials that are defined as materials having at least one dimension in the 1 to 100 nm size range.

Nanomaterials have specific properties not exhibited by dissolved compounds. For instance, unlike organic compounds, CNTs cannot dissolve in organic solvents or water [16] and the dimensions of CNTs are not small enough to diffuse into SOMs and polymers. Surface charge, Hamaker constant, and adsorption of low molecular weight organic compounds have to be considered when studying CNT interactions with surfaces, as well as the aggregation of CNTs with themselves (homoaggregation) or other suspended particles (heteroaggregation).

Soils also contain mobile organic molecules that usually have a relatively low enough molecular weight to behave similarly to dissolved molecules. These carbon-based molecules are often termed dissolved organic matter (DOM) to distinguish them from non-mobile organic matter, here referred to as SOM. Even though this distinction is often operationally based on a 0.45 μm filtration, or in this study based on a centrifugation step, previous studies have shown that adsorption of DOM on CNTs usually creates a thermodynamically more favorable hydrophilic surface thus preventing hydrophobic interactions and electrosterically stabilize CNT suspensions against deposition [17], homoaggregation [9, 18-21] and heteroaggregation [22], effectively increasing their potential transport in porous media and

thus also their bioavailability [23]. Interactions with SOM most often reduce the transport of CNTs drastically in soils, because SOM may constitute preferential binding sites for CNTs that can experience hydrophobic attractions [24], contrary to inorganic nanomaterials. However, SOM can release DOM molecules and adsorption of DOM can in some cases increase aggregation of incompletely coated CNTs by bridging flocculation, in some cases assisted by Ca^{2+} forming ion bridges between coating molecules [23]. It has indeed been found that CNT transport in natural soils is very limited [25], whereas CNT transport in simple sand columns can be very high [26, 27]. SOM are often composed of macromolecules, i.e. molecules with a weight too high to occur as truly dissolved carbon-based molecules. Considering the variability of organic molecules in natural systems, a systematic study on the effect of such macromolecules on CNT fate is urgently needed to improve ecotoxicological risk predictions of CNTs. Because of the heterogeneous nature of SOM macromolecules, it is difficult to describe their molecular structure. Therefore, macromolecules that are either natural (lignin, chitin and cellulose) or synthetic, with a clearly defined molecular structure, are commonly used as model DOMs [14-16].

In this study, we screened the effect of 16 macromolecules as models for SOM: 3 humic acids (HAs), 3 biopolymers and 10 polymers on the fate of ^{14}C -labeled multiwall carbon nanotubes (MWCNTs) using a batch method. The selected molecules encompassed a range of surface properties and molecular weights. The specific objectives of this study were to find the favorable and unfavorable macromolecule properties for MWCNT retention; and to determine the relative strength of each property for MWCNT retention on macromolecules. During the batch method used in this study, interactions between CNTs and macromolecules are allowed for a given time during which larger MWCNT aggregates may be formed that are large enough to be sedimented during a centrifugation step. When investigating the interaction of nanomaterials with large solid surfaces, the term deposition is used, whereas the term aggregation is reserved for suspended particles interacting with each other. Although the distinction between adsorption and deposition is not always clear, deposition is reserved for kinetic interactions, the rates of which are determined by the balance of surface potentials caused by Van der Waals and electrostatic attraction forces [28]. If deposition occurs in the primary energy minimum, it is considered permanent, albeit resuspension can occur in exceptional circumstances (e.g. a drastic drop in ionic strength) [29]. Deposition, however, often occurs in the secondary energy minimum from which resuspension is more frequently possible by simple diffusion, but even more so by chemical and hydraulic perturbations [30]. The co-occurrence of deposition and resuspension can on the long-term thus lead to a pseudo-equilibrium situation [31]. The difference between this pseudo-equilibrium and a real adsorption equilibrium is that the pseudo-equilibrium emerges from two mechanisms, deposition and resuspension, that are controlled by entirely different parameters, whereas adsorption and desorption are both controlled by thermodynamics and the same activation energy. Moreover, there is always a subpopulation of deposited material that is not resuspended, because it is irreversibly attached. The term deposition was therefore used to designate the retention of MWCNT by macromolecules, whereas resuspension was used for the release of MWCNT by macromolecules.

2. Materials and Methods

2.1 Macromolecules

One HA was extracted from a peat soil in Michigan. The other two HAs were extracted from a peat soil in Amherst, Massachusetts. The extraction procedure was previously described in detail [11, 12]. In brief, soil was progressively extracted seven times with 0.1 mol L^{-1} $\text{Na}_4\text{P}_2\text{O}_7$ and six times with 0.1 mol L^{-1} NaOH . The first fraction of Michigan peat soil (HA1), the second (HA2) and fifth (HA3) fractions of Amherst peat soil were used in our study. Lignin was purchased from Sigma-Aldrich Co. Cellulose was bought from Fisher Scientific Co. Chitin was obtained from MP Biomedicals Inc. Seven types of polyethylene, obtained from Sigma-Aldrich Chemical Co., with different molecular weights (MW) and densities (PE1: high density; PE2: 3,000,000 to 6,000,000 molecular weight (MW); PE3: 35,000 MW; PE4: 4,000 MW; PE5: high density; PE6: low density; PE7: linear low density), two types of polystyrene with different molecular structures (one that was linear (PS1) and a second that was 20% cross-linked (PS2)) and an oxygen-containing polymer poly(2,6-dimethyl-1,4-phenyleneoxide) (PPO) were selected as simplified models for SOMs. Additional characterization of the 10 polymers was described in our previous study [32]. Polymers originally in pellet form were ground to fine powers (diameter < 0.15 mm) using an ultra-centrifugation grinding miller (ZM200, Retsch Germany), freeze-dried, and stored. To minimize potential ion release, all macromolecules were washed by distilled water until a final conductivity value of the eluent below 1.0 $\mu\text{S/cm}$ was obtained by the conductivity analyzer (DDS-307, Jingke Shanghai Co.). This procedure ensured that the macromolecules did not increase the solution ionic strength, a parameter known to impact MWCNT retention [33].

2.2 MWCNT

^{14}C -labeled MWCNTs were synthesized by a modified chemical vapor deposition (CVD) [24, 34, 35]. The pristine ^{14}C -MWCNTs were purified through bath sonication with concentrated hydrochloric acid (11.1 mol L^{-1}) for 1 h. Then, the purified MWCNTs were functionalized using an acid mixture of concentrated sulfuric (14.8 mol L^{-1}) and nitric (15.6 mol L^{-1}) acids by a 3:1 (volume:volume) ratio to make them stable in water [9, 36]. The physicochemical properties of MWCNTs have been described previously [9, 36]. In brief, the functionalized MWCNTs after acid treatment were $(99.7 \pm 0.2) \%$ pure with respect to metal catalyst impurities on a mass basis, and had a $111 \text{ m}^2/\text{g}$ specific surface area and a specific radioactivity of 0.1 mCi/g . Additional characterization is provided in the Supporting Information (Figure S1).

A stable stock suspension of MWCNTs was then obtained by dispersing 100 mg MWCNTs into 1 L of de-ionized water via ultrasonication (200 W; Cole-Parmer CV33) for 2 h. The suspension was kept at room temperature for at least 6 h before use. To verify the suspension was stable, the initial concentration of MWCNTs was determined before use every time by liquid scintillation counting (LSC; Benchman [Fullerton, CA] LS6500) and was $74.1 \pm 1.0 \text{ mg L}^{-1}$. The electrophoretic mobility (μ) of the sonicated MWCNTs was $-0.57 \text{ cm}^2 \text{ V}^{-1} \text{ s}^{-1} \pm 0.06 \text{ cm}^2 \text{ V}^{-1} \text{ s}^{-1}$ (uncertainty values always indicate standard deviation values) and $-0.89 \text{ cm}^2 \text{ V}^{-1} \text{ s}^{-1} \pm 0.03 \text{ cm}^2 \text{ V}^{-1} \text{ s}^{-1}$ at $\text{pH}=4$ and $\text{pH}=7$ in $4 \text{ mmol L}^{-1} \text{ Na}^+$ background

solution, respectively (90Plus, Brookhaven), results similar to those obtained previously for these MWCNTs [9]. The calculation of zeta potential values from electrophoretic mobility measurements typically uses the Henry equation and the Smoluchowski approximation which assumes spherical particles [3]. Therefore, this approach should not be used for non-spherical nanoparticles such as CNTs, and we report electrophoretic mobility values instead [3]. In a previous study wherein the acid-treated MWCNTs produced by this synthesis process were sonicated for 6 h, the surface oxygen content increased from 7.4% to 8.6% [9], thus suggesting that there may be a minor increase in the surface oxygen content after sonication for the 2 h period used in this study. The average diameter of the acid-treated MWCNTs after sonication for 6 h was (36.5 ± 12.7) nm ($n = 80$) ranging from 20 nm to 90 nm, and the average length of MWCNTs was (353 ± 452) nm ($n = 836$; see Figure S1 part c for histogram) [9]. Our previous study also showed that sonication for 6 h did not change the amount of metal catalyst remaining in the functionalized nanotube samples and it did not produce an amorphous carbon peak according to thermogravimetric analysis [9].

2.3 Macromolecule Characterization

Elemental compositions of C, H, N (using oxygen) and O (using helium) were measured at 1150 °C with an elemental analyzer (MicroCube, Elementar, Germany). Surface elemental composition was obtained using an AXIS-Ultra X-ray Imaging Photoelectron Spectrometer (Kratos Analytical Ltd., UK) with a monochromatic Al K α radiation source operated at 225 W, 15 mA, and 15 KV. Electrophoretic mobility (μ) of molecules was measured using a Zeta Potential Analyzer (90Plus, Brookhaven). Surface areas (SA) of the macromolecules were measured using Autosorb-1 Surface Area Analyzer (Quantachrome, USA). The SA of macromolecules was derived from N₂ sorption-desorption isotherms using the BET method. The solid-state cross-polarization magic angle spinning ¹³C NMR spectra of the macromolecules were obtained using a Bruker DRX-400 spectrometer operated at a ¹³C frequency of 100.36 MHz and a magic-angle-spinning rate of 8.0 kHz. The amount of DOM released by the macromolecules was operationally defined as the carbon concentration remaining in suspension after centrifugation at 3500 *g* for 1 min. The DOM concentration was determined after incubation for 7 d at their corresponding experimental pH and at a sodium concentration of 4 mmol L⁻¹ using a total organic carbon (TOC) analyzer (TOC-L, SHIMADZU). Buffers were not used because the sodium acetate buffer, which was used in the deposition experiments for pH stabilization, would increase the TOC measurement. All macromolecule property measurements were made in triplicate.

2.4 Deposition Experiments

MWCNT retention experiments were conducted using a batch technique at (25 ± 1) °C as described previously [9, 36]. Five mg of a macromolecule was added into 8 mL background solutions containing 4 mmol L⁻¹ Na⁺ at pH 4 using a 4 mM sodium acetate buffer for HAS and pH 7 using a 4 mM sodium phosphate buffer with an initial concentration of MWCNT that ranged from (0 to 50) mg L⁻¹. The choice of sodium concentration (4 mmol L⁻¹) and pH 7 for the background solution was based on environmental relevance. All three HAS were easily suspended at pH 7, eliminating the potential for MWCNT deposition to unsuspended HAs. In this study, we tested a single solution pH and ionic strength to focus exclusively on the impact of macromolecule properties on MWCNT deposition. The mixtures were shaken

at 150 rpm for 7 d and then left without shaking for another 7 d. Both shaking and settling steps were conducted in dark. Preliminary experiments showed that there was no significant difference between 7 and 12 days shaking indicating an apparent equilibrium had been reached (Figure S2), which is consistent with our previous studies [9, 36]. Samples were centrifuged at 3500 *g* for 1 min to sediment suspended macromolecules. Absorbance measurements at 800 nm (Agilent 8453 UV spectrophotometer) of control samples (containing only solid macromolecules) after centrifugation indicated removal of suspended macromolecule to below the detection limit. Three mL of supernatant for MWCNT samples was then mixed with 3 mL of scintillation cocktail (Ultima gold XR, Fisher Scientific, PA) for liquid scintillation counting (LSC; Benchman [Fullerton, CA] LS6500). The detection limit for LSC analysis of C-14 MWCNTs was 50 $\mu\text{g L}^{-1}$. Supernatants containing the same concentration of ^{14}C -MWCNTs with and without DOM were analyzed using LSC to test for matrix effects, but no significant difference was found. Because the release of DOM could influence MWCNT deposition on peat [7], the potential for each macromolecule to release detectable concentrations of DOM using TOC analysis was also measured as described above. For macromolecules with DOM release (HAs, Lignin, Cellulose and Chitin), the macromolecules were incubated at the same solid/solution ratio and with the same pH and ionic strength as for the experimental group for 7 d and then centrifuged at 3500 *g* for 1 min to remove the solid macromolecule. MWCNTs were then mixed with the supernatant of these experiments to assess the effect of released DOM on MWCNT settling. For macromolecules without detectable DOM concentrations (PEs, PSs and PPO), settling in samples with the same solution as that in the retention experiments but without macromolecules was used to estimate MWCNT settling during the batch experiments. All experiments were repeated at least twice.

The total mass of MWCNTs that had deposited on macromolecule and/or settled during the experiment, M_s (mg) was calculated by mass balance as follows:

$$M_s = (C_0 - C_{aq}) V \quad (1)$$

where C_0 is the initial mass concentration of MWCNTs (mg L^{-1}); C_{aq} is the aqueous phase mass concentration of MWCNTs (mg L^{-1}); and V is sample volume (0.008 L). The deposited mass concentration (mg kg^{-1}) of MWCNTs (q_s) is:

$$q_s = (M_{ss} - M_{sc}) / D \quad (2)$$

where M_{ss} is the total mass of MWCNTs that includes settling and retention on macromolecules (mg); M_{sc} is the total mass of settled MWCNTs (mg); and D is the dosage of macromolecules (0.005 g). M_{sc} is determined from experiments described above which assessed the decrease in the aqueous phase MWCNT from settling in the absence of interactions with a solid phase. These measurements were made with DOM for macromolecules (HAs, Lignin, Cellulose and Chitin) that released DOM or with only water for all other macromolecules (PEs, PSs and PPO).

2.5 Redispersion Experiments

Redispersion experiments were done immediately after the 14 d deposition period to assess the potential for resuspension of MWCNTs that had been deposited or settled out of the dispersion. Six mL of suspension was removed from the vials and the same volume of background solution (containing the same concentrations of DOM and Na⁺ ion) was added. The vials were then shaken on the rotary shaker at 150 rpm for another 7 d and then left in the dark for 7 d. The vials were subsequently centrifuged for 1 min at 3500 g and the MWCNT concentration in supernatant was analyzed by LSC as described above.

2.6 Statistical Evaluation

Multiple linear regression analysis combined with path analysis was conducted using SPSS 18.0. Kolmogorov-Smirnov test and Q-Q plots were used for data normality testing using SPSS. Because of the non-normality of data for macromolecule properties as indicated by Kolmogorov-Smirnov test, all macromolecule properties were log-transformed to meet the normality criteria (Table S1). The Q-Q plots for each log-transformed macromolecule properties are also provided in Figure S3. The value of VIF (Variance Inflation Factor) of logP, logA, logS, logD and log Z were 3.008, 1.694, 1.432, 3.188 and 1.289, respectively, suggesting insignificant effects of multicollinearity. The applicability domain of multiple linear regression result was verified by the leverage approach [37, 38] using the plot of standardized residuals versus leverages (hat diagonals), i.e. the Williams plot. The leverage of a compound is defined as

$$h_i = x_i^T (X^T X)^{-1} x_i \quad (3)$$

where x_i is the descriptor vector of the considered compound and X is the descriptor matrix derived from the training set descriptor values. The warning leverage (h^*) is defined as $h^* = 3(N+1)/n$, where N is the number of independent variables in the model ($N = 6$) and n is the number of training compounds ($n = 12$ in this study). If the leverage of the compound $h_i > h^*$, it suggests that the compound is very influential on the model. If the standardized residual of a compound is greater than three standard deviation units ($\pm 3\sigma$), the compound will be regarded as an outlier.

3. Results and Discussion

3.1 Macromolecule Characterization

Comprehensive characterization of the different macromolecules using multiple techniques indicated a diverse distribution of macromolecule properties. HAs and biopolymers (lignin, cellulose and chitin) showed substantially different surface and bulk polarity values, suggesting heterogeneity of the macromolecules (Table 1). Surface polarity of PEs, PSs and PPO were slightly different from their bulk polarity which was most likely due to partial oxidation and/or moisture adsorption (Table 1). Candidate physicochemical properties of the macromolecule that may have relationship with deposition are summarized in Table 2. The aromaticity ranged from 0 to 75 %; SA ranged from 0.2 to 70.2 m² g⁻¹; the amount of DOM

released from macromolecules in solution ranged from 0 to 44.3 mg C L⁻¹; and the electrophoretic mobility of macromolecules in solution ranged from $-1.34 \pm 0.09 \text{ cm}^2 \text{ V}^{-1} \text{ s}^{-1}$ to $-4.29 \pm 0.09 \text{ cm}^2 \text{ V}^{-1} \text{ s}^{-1}$.

3.2 Effect of DOM

In the absence of DOM, only $16.2 \% \pm 4.43 \%$ ($n = 22$) of MWCNTs settled out of the dispersion (using data from settling at pH 4 and 7), suggesting limited homoaggregation of MWCNT suspension in the solutions tested (Figure 1a), probably because the ionic strength tested (4 mM NaCl) is far below critical coagulation concentrations of oxidized MWCNTs that are of the order of 90 mM NaCl at pH 6 [39]. The amount of settled MWCNTs at pH 4 ($18.0 \% \pm 4.93 \%$) was slightly higher than at pH 7 ($14.5 \% \pm 2.59 \%$) likely due to the less negative MWCNT electrophoretic mobility at pH 4. The amount of settling dramatically decreased in the presence of DOM derived from HA as seen by the more negative slopes compared to the blanks of M_{sc} with C_{aq} (Figure 1a). Conversely, inclusion of DOM from the chitin and cellulose caused more positive M_{sc} to C_{aq} slopes, indicating more settling occurred, compared to the pH = 7 blanks. Chitin and cellulose are not readily soluble at pH = 7, so the operationally defined DOM emerging from these macromolecules is most likely suspended low molecular weight fibres that were too short to settle during centrifugation. HA that dissolves at pH = 4 still possesses significant negative charge [40]. HA-DOM is thus known to decrease collision efficiency electrosterically of MWCNTs drastically [9, 41, 42], whereas MWCNT apparently heteroaggregates with cellulose and chitin fibres, possibly because of the low surface charge density often found on these macromolecules [43], and this heteroaggregation may lead to settling.

3.3 Deposition

The deposited functionalized MWCNTs mass increased linearly with total MWCNT mass (Figure 1b, 1c and Tables S2). Such linear behavior suggests the absence of blocking (i.e. previously deposited MWCNT decrease deposition rates by repelling MWCNT) or ripening (i.e. previously deposited MWCNT enhance deposition rates by attracting MWCNT).

Largely due to the challenge of quantifying CNTs in solid samples [9, 10], there are no quantitative studies to our knowledge on CNTs redispersion after deposition. This investigation thus marks the first assessment of this topic. However, suspended concentrations could not be used to accurately evaluate dispersion, because it was impossible to remove all MWCNTs from the suspension before starting the redispersion experiment. No significant change was observed in the solid phase concentration after the redispersion period for any of the 16 macromolecules tested (Figure 2). This observation suggests that MWCNT resuspension is minimal and deposition is largely irreversible. Irreversible deposition kinetics are often assumed first order according to

$$dM_s/dt = kn_{aq} \quad (4)$$

where k is the first-order rate coefficient and n is the number concentration of MWCNT. All deposition experiments were run with the same time T so equation (4) solves as $M_s/n_{aq} = kT$.

The retention coefficient [8], i.e. the mass of deposited MWCNT per mass of macromolecule, divided by the suspended mass, k_r ($L g^{-1}$) was determined by fitting linear curves to concentration dependent relations of q_s :

$$q_s = k_r C_{aq} \quad (5)$$

The retention coefficient, also called the distribution coefficient [44], if determined under exactly the same hydrodynamic conditions, is proportional to differences in the deposition rate constant. Differences in k_r should thus reflect physicochemical factors determining differences in deposition rate [45].

It was difficult to find a relationship between a single macromolecule property (surface and bulk (O+N)/C, aromaticity, SA, DOM, or the difference between electrophoretic mobility of macromolecules and MWCNTs (hereafter referred to as Z) and k_r , as indicated by low correlation coefficients R^2 (0.037, 0.127, 0.000, 0.002, 0.092 and 0.004) when trying to fit a linear regression to this data (Figure S4). A linear relationship was observed between the retention coefficients and the settling rates (Figure S5). This relation suggests settling and retention are caused by similar mechanisms, i.e. deposition of MWCNT. When the DOM helps the MWCNTs stay dispersed in the aqueous suspension, they are less likely to interact with solid particles and sediment. Conversely, DOM from the chitin sample caused increased settling compared to the water only solution and this sample also had the highest retention coefficients. A multiple linear regression approach was applied to further study the relationship between macromolecule properties and retention.

3.4 Multiple linear Regression Study

Multiple linear regression has been widely used in environmental chemistry and contaminant fate modeling [37, 38, 46-52]. Similarly, nanomaterial retention coefficients have been correlated with properties of natural soils to elucidate the most important properties affecting nanomaterial deposition [53, 54]. The correlation of k_r with the macromolecule properties was established by multiple linear regression analysis of the [k_r , log surface (O+N)/C, log aromaticity, log SA, log DOM and log Z] matrix. This yielded the following equation

$$k_r = -0.190 - 0.054 \log P + 0.147 \log A - 0.386 \log S - 0.057 \log D + 1.694 \log Z, \quad n=16, R^2=0.73$$

(6)

where P is surface (C+O)/N of macromolecules; A represents macromolecule aromaticity; S is macromolecule surface area; and D represents released concentration of DOM released from the macromolecules. Analysis of variance results suggested that the regression equation had statistical significance (Table S3). The robustness of Equation (6) was evaluated through an initial two step development: 1) splitting the data into training and validation sets (see Table S2) and 2) validating the data via internal and external certification [38, 55, 56]. To split the data into training and validation sets, we first sorted the 16

macromolecules based on decreasing maximum k_r value. Second, the data were split into three sets: chitin and PS2 which have the highest and the lowest k_r value were grouped into the validation set V_2 to represent the macromolecules that are not within the range of the training set. The remaining 14 macromolecule molecules were split into two sets: training set (T) and the validation set (V_1) following pattern T-T-T-T- V_1 -T-T-T-T- V_1 -T-T-T-T to ensure the V_1 set is evenly distributed in the training set. The predicted versus measured k_r values of the training set and validation set 1 and 2 are shown in Figure 3a. All data are close to the 1:1 line, suggesting the robustness of equation (6). The applicability domain of the model was verified using a William plot (Figure 3b). All the training and validation compounds in various equilibrium concentrations are within the chemical domain, suggesting that there are no outliers and the predictive capacity of the model is reliable. We also used bulk (O+N)/C value instead of surface (O+N)/C for the multiple linear regression. When using the bulk (O+N)/C values, the regression coefficient R^2 decreased to 0.55, a value much lower than when using the surface (O+N)/C values (0.73). This suggests that surface polarity rather than bulk polarity more strongly impacted MWCNT retention.

3.5 Path Analysis Study

Equation (6) cannot reveal the relative contribution of each macromolecule property on MWCNT retention. This is because each macromolecule property has a different unit. Besides, macromolecule properties not only affect MWCNT retention through a direct interaction, but also influence retention indirectly via affecting other macromolecule properties (Table 3). Path analysis was therefore employed to estimate the relative strengths of direct and indirect interactions among variables (Table 4) [57].

Sorbent aromaticity (log A, 0.258) and surface polarity (log P, 0.178) were the two most important macromolecule properties for MWCNT retention. The aromatic moieties in the macromolecules could interact with benzene rings in MWCNTs, which would be expected to result in strong π - π interactions. Macromolecules with high aromaticity would be expected to thus favor CNT retention. Due to strong van der Waals and hydrophobic forces, MWCNTs are prone to form bundles and agglomerate in water, making the hydrophilic groups facing to water [58]. The abundant surface oxygen-containing group on the MWCNTs (8.6 % as measured by X-ray photoelectron spectroscopy analysis [9]) may act as H-bonding donors to build hydrogen bonding with the O/N-containing polar moieties on macromolecule surface, attracting MWCNT from aqueous phase to the macromolecule particles [59-61].

Increasing surface area (logS, -0.206) had the most substantial effect among the macromolecule properties measured for decreasing MWCNT retention. This was unexpected, because one would assume that the higher the surface area of macromolecule was, the stronger MWCNT retention would be. The macromolecule surface area values come mainly from two contributions: macromolecule pore surface area and macromolecule outer surface area. MWCNTs only have one dimension in nanoscale and their length was on average approximately an order of magnitude larger (353 nm on average) [36] than their diameters which likely inhibited them from penetrating into the micropores of macromolecules. Thus, only the contribution of macromolecule pores (diameter > MWCNT

diameter) and the outer surface of macromolecules have a retention capacity for the MWCNTs. The increased electrostatic repulsion caused by the difference in electrophoretic mobility between MWCNTs and macromolecules (Z) also had a negative effect on retention ($\log Z$, -0.094). This repulsive effect may be from both the MWCNTs and macromolecules having negative electrophoretic mobilities while positively charged nanomaterials may be attracted to these same polymers (Table 2).

4. Summary

For all 16 macromolecules, the amount of functionalized MWCNTs in solid phase remained unchanged after redispersion (Figures S5), indicating that irreversible deposition of MWCNTs occurred on the macromolecules studied. Path analysis revealed that irreversible deposition of MWCNT can mostly be explained by polar interactions with the macromolecule surfaces. It is noteworthy that solution conditions (i.e. ionic strength, pH) have not been considered in this study, although ionic strength has been shown to impact MWCNT retention by clays and peat [9, 36]. However, the impact of pH will be limited given that the pK_a of most CNTs occurs at pH values irrelevant for most environmental systems (> 11) [62]. The retention and redispersion results obtained in this study help explain the limited transport distances encountered in natural soils containing soil organic matter [25]. Our findings on the relative strength of macromolecule properties for CNT retention provide information on selection of carbon based molecules for removal of MWCNTs from wastewater and provide a method for measuring CNT interactions with macromolecules.

Supplementary Material

Refer to Web version on PubMed Central for supplementary material.

Acknowledgements

This work was in part supported by the Hundreds Talents Program of Chinese Academy of Sciences, USDA-AFRI Hatch program (MAS 00475), NSFC (41328003) and the 111 project (B14001) and Open Foundation of State Key Laboratory of Environmental Criteria and Risk Assessment, Chinese Research Academy of Environmental Sciences (SKLECRA2015OFP10). Certain commercial equipment or materials are identified in this article in order to specify adequately the experimental procedure. Such identification does not imply recommendation or endorsement by the National Institute of Standards and Technology, nor does it imply that the materials or equipment identified are necessarily the best available for the purpose.

REFERENCES

1. Porter AE, Gass M, Muller K, Skepper JN, Midgley PA, Welland M. Direct imaging of single-walled carbon nanotubes in cells. *Nat Nanotechnol.* 2007; 2:713–7. [PubMed: 18654411]
2. Lam CW, James JT, McCluskey R, Arepalli S, Hunter RL. A review of carbon nanotube toxicity and assessment of potential occupational and environmental health risks. *Crit Rev Toxicol.* 2006; 36:189–217. [PubMed: 16686422]
3. Petersen EJ, Henry TB. Methodological considerations for testing the ecotoxicity of carbon nanotubes and fullerenes: Review. *Environ Toxicol Chem.* 2012; 31:60–72. [PubMed: 21994158]
4. Godwin H, Nameth C, Avery D, Bergeson LL, Bernard D, Beryt E, et al. Nanomaterial categorization for assessing risk potential to facilitate regulatory decision-making. *ACS Nano.* 2015; 9:3409–3417. [PubMed: 25791861]

5. Gottschalk F, Sonderer T, Scholz RW, Nowack B. Modeled environmental concentrations of engineered nanomaterials (TiO₂, ZnO, Ag, CNT, Fullerenes) for different regions. *Environ Sci Technol.* 2009; 43:9216–22. [PubMed: 20000512]
6. Wang YF, Westerhoff P, Hristovski KD. Fate and biological effects of silver, titanium dioxide, and C-60 (fullerene) nanomaterials during simulated wastewater treatment processes. *J Hazard Mater.* 2012; 201:16–22. [PubMed: 22154869]
7. Kiser MA, Ladner DA, Hristovski KD. Nanomaterial transformation and association with fresh and freeze-dried wastewater activated sludge: Implications for testing protocol and environmental fate. *Environ Sci Technol.* 2012; 46:7046–53. [PubMed: 22320890]
8. Cornelis G, Kirby JK, Beak D, Chittleborough D, McLaughlin MJ. A method for determining the partitioning of manufactured silver and cerium oxide nanoparticles in soil environments. *Environ Chem.* 2010; 7:298–308.
9. Zhang LW, Petersen EJ, Huang QG. Phase distribution of C-14-labeled multiwalled carbon nanotubes in aqueous systems containing model solids: Peat. *Environ Sci Technol.* 2011; 45:1356–62. [PubMed: 21222444]
10. Petersen EJ, Pinto RA, Zhang LW, Huang QG, Landrum PF, Weber WJ. Effects of polyethyleneimine-mediated functionalization of multi-walled carbon nanotubes on earthworm bioaccumulation and sorption by soils. *Environ Sci Technol.* 2011; 45:3718–24. [PubMed: 21434629]
11. Kang SH, Xing BS. Phenanthrene sorption to sequentially extracted soil humic acids and humins. *Environ Sci Technol.* 2005; 39:134–40. [PubMed: 15667087]
12. Wang XL, Guo XY, Yang Y, Tao S, Xing BS. Sorption mechanisms of phenanthrene, lindane, and atrazine with various humic acid fractions from a single soil sample. *Environ Sci Technol.* 2011; 45:2124–30. [PubMed: 21341701]
13. Yang Y, Shu L, Wang XL, Xing BS, Tao S. Impact of de-ashing humic acid and humin on organic matter structural properties and sorption mechanisms of phenanthrene. *Environ Sci Technol.* 2011; 45:3996–4002. [PubMed: 21469711]
14. Xing BS, McGill WB, Dudas MJ, Maham Y, Hepler L. Sorption of phenol by selected biopolymers - isotherms, energetics, and polarity. *Environ Sci Technol.* 1994; 28:466–73. [PubMed: 22165882]
15. Wang XL, Xing BS. Importance of structural makeup of biopolymers for organic contaminant sorption. *Environ Sci Technol.* 2007; 41:3559–65. [PubMed: 17547178]
16. Petersen EJ, Huang QG, Weber WJ. Relevance of octanol-water distribution measurements to the potential ecological uptake of multi-walled carbon nanotubes. *Environ Toxicol Chem.* 2010; 29:1106–12. [PubMed: 20821546]
17. Wang P, Shi Q, Liang H, Steuerman DW, Stucky GD, Keller AA. Enhanced environmental mobility of carbon nanotubes in the presence of humic acid and their removal from aqueous solution. *Small.* 2008; 4:2166–70. [PubMed: 19058159]
18. Lin DH, Liu N, Yang K, Xing BS, Wu FC. Different stabilities of multiwalled carbon nanotubes in fresh surface water samples. *Environ Pollut.* 2010; 158:1270–4. [PubMed: 20171769]
19. Schwyzer I, Kaegi R, Sigg L, Nowack B. Colloidal stability of suspended and agglomerate structures of settled carbon nanotubes in different aqueous matrices. *Water Res.* 2013; 47:3910–20. [PubMed: 23582307]
20. Schwyzer I, Kaegi R, Sigg L, Smajda R, Magrez A, Nowack B. Long-term colloidal stability of 10 carbon nanotube types in the absence/presence of humic acid and calcium. *Environ Pollut.* 2012; 169:64–73. [PubMed: 22683482]
21. Schwyzer I, Kaegi R, Sigg L, Magrez A, Nowack B. Influence of the initial state of carbon nanotubes on their colloidal stability under natural conditions. *Environ Pollut.* 2011; 159:1641–8. [PubMed: 21435759]
22. Huynh KA, McCaffery JM, Chen KL. Heteroaggregation of Multiwalled Carbon Nanotubes and Hematite Nanoparticles: Rates and Mechanisms. *Environ Sci Tech.* 2012; 46:5912–20.
23. Cornelis G, Hund-Rinke KM, Kuhlbusch T, Van den Brink N, Nickel C. Fate and bioavailability of engineered nanoparticles in soils: a review. *Crit Rev Env Sci Technol.* 2014; 44:2720–64.

24. Petersen EJ, Zhang LW, Mattison NT, O'Carroll DM, Whelton AJ, Uddin N, et al. Potential release pathways, environmental fate, and ecological risks of carbon nanotubes. *Environ Sci Technol*. 2011; 45:9837–56. [PubMed: 21988187]
25. Kasel D, Bradford SA, Šim nek J, Pütz T, Vereecken H, Klumpp E. Limited transport of functionalized multi-walled carbon nanotubes in two natural soils. *Environ Pollut*. 2013; 180:152–8. [PubMed: 23770315]
26. Tian YA, Gao B, Ziegler KJ. High mobility of SDBS-dispersed single-walled carbon nanotubes in saturated and unsaturated porous media. *J Hazard Mater*. 2011; 186:1766–72. [PubMed: 21236566]
27. O'Carroll DM, Liu X, Mattison NT, Petersen EJ. Impact of diameter on carbon nanotube transport in sand. *J Coll Interf Sci*. 2013; 390:96–104.
28. Elimelech, M.; Gregory, J.; Jia, X.; Williams, RA. Particle deposition and aggregation: measurement, modelling and simulation. Butterworth Heinemann; Woburn: 1995.
29. Mattison NT, O'Carroll DM, Rowe RK, Petersen EJ. Impact of porous media grain size on the transport of multi-walled carbon nanotubes. *Environ Sci Technol*. 2011; 45:9765–75. [PubMed: 21950836]
30. Ryan JN, Elimelech M. Colloid mobilization and transport in groundwater. *Colloid Surface A*. 1996; 107:1–56.
31. Degueldre C, Aeberhard P, Kunze P, Bessho K. Colloid generation/elimination dynamic processes: Toward a pseudo-equilibrium? *Colloid Surface A*. 2009; 337:117–26.
32. Guo XY, Wang XL, Zhou XZ, Kong XZ, Tao S, Xing BS. Sorption of four hydrophobic organic compounds by three chemically distinct polymers: Role of chemical and physical composition. *Environ Sci Technol*. 2012; 46:7252–9. [PubMed: 22676433]
33. Smith B, Yang J, Bitter JL, Ball WP, Fairbrother DH. Influence of Surface Oxygen on the Interactions of Carbon Nanotubes with Natural Organic Matter. *Environ Sci Tech*. 2012; 46:12839–47.
34. Petersen EJ, Huang QG, Weber WJ. Bioaccumulation of radio-labeled carbon nanotubes by *Eisenia foetida*. *Environ. Sci. Technol*. 2008; 42:3090–5. [PubMed: 18497171]
35. Petersen EJ, Huang QG, Weber WJ. Ecological uptake and depuration of carbon nanotubes by *Lumbriculus variegatus*. *Environ Health Perspect*. 2008; 116:496–500. [PubMed: 18414633]
36. Zhang LW, Petersen EJ, Zhang W, Chen YS, Cabrera M, Huang QG. Interactions of C-14-labeled multi-walled carbon nanotubes with soil minerals in water. *Environ Pollut*. 2012; 166:75–81. [PubMed: 22481179]
37. Xia XR, Monteiro-Riviere NA, Riviere JE. An index for characterization of nanomaterials in biological systems. *Nat Nanotechnol*. 2010; 5:671–5. [PubMed: 20711178]
38. Zhao Q, Yang K, Li W, Xing BS. Concentration-dependent polyparameter linear free energy relationships to predict organic compound sorption on carbon nanotubes. *Sci Rep*. 2014; 4:1–7.
39. Smith B, Wepasnick K, Schrote KE, Bertele AH, Ball WP, O'Melia C, et al. Colloidal Properties of Aqueous Suspensions of Acid-Treated, Multi-Walled Carbon Nanotubes. *Environ Sci Tech*. 2009; 43:819–25.
40. Hosse M, Wilkinson KJ. Determination of electrophoretic mobilities and hydrodynamic radii of three humic substances as a function of pH and ionic strength. *Environ Sci Tech*. 2001; 35:4301–6.
41. Chappell MA, George AJ, Dontsova KM, Porter BE, Price CL, Zhou PH, et al. Surfactive stabilization of multi-walled carbon nanotube dispersions with dissolved humic substances. *Environ Pollut*. 2009; 157:1081–7. [PubMed: 19000646]
42. Chang X, Henderson WM, Bouchard DC. Multiwalled carbon nanotube dispersion methods affect their aggregation, deposition, and biomarker response. *Environ Sci Tech*. 2015; 49:6645–6653.
43. Budd J, Herrington TM. Surface charge and surface area of cellulose fibres. *Colloids and Surfaces*. 1989; 36:273–88.
44. Barton LE, Therezien M, Auffan M, Bottero JY, Wiesner MR. Theory and methodology for determining nanoparticle affinity for heteroaggregation in environmental matrices using batch measurements. *Environ Eng Sci*. 2014; 31:421–7.
45. Cornelis G. Fate descriptors for engineered nanoparticles: the good, the bad, and the ugly. *Environmental Science: Nano*. 2015; 2:19–26.

46. Nguyen TH, Goss KU, Ball WP. Polyparameter linear free energy relationships for estimating the equilibrium partition of organic compounds between water and the natural organic matter in soils and sediments. *Environ Sci Technol.* 2005; 39:913–24. [PubMed: 15773462]
47. Schuurmann G, Ebert RU, Kuhne R. Prediction of the sorption of organic compounds into soil organic matter from molecular structure. *Environ Sci Technol.* 2006; 40:7005–11. [PubMed: 17154008]
48. Gotz CW, Scheringer M, Macleod M, Roth CM, Hungerbuhler K. Alternative approaches for modeling gas-particle partitioning of semivolatile organic chemicals: Model development and comparison. *Environ Sci Technol.* 2007; 41:1272–8. [PubMed: 17593730]
49. Endo S, Grathwohl P, Haderlein SB, Schmidt TC. Compound-specific factors influencing sorption nonlinearity in natural organic matter. *Environ Sci Technol.* 2008; 42:5897–903. [PubMed: 18767642]
50. Zhu RL, Chen WX, Shapley TV, Molinari M, Ge F, Parker SC. Sorptive characteristics of organomontmorillonite toward organic compounds: a combined LFERs and molecular dynamics simulation study. *Environ Sci Technol.* 2011; 45:6504–10. [PubMed: 21721563]
51. Abraham MH, Le J. The correlation and prediction of the solubility of compounds in water using an amended solvation energy relationship. *J Pharm Sci.* 1999; 88:868–80. [PubMed: 10479348]
52. Zhu LZ, Yang K, Lou BF, Yuan BH. A multi-component statistic analysis for the influence of sediment/soil composition on the sorption of a nonionic surfactant (Triton X-100) onto natural sediments/soils. *Water Res.* 2003; 37:4792–800. [PubMed: 14568066]
53. Cornelis G, Doolette C, Thomas M, McLaughlin MJ, Kirby JK, Beak D, et al. Retention and dissolution of engineered silver nanoparticles in natural soils. *Soil Sci Soc Am J.* 2012; 76:891–902.
54. Cornelis G, Ryan B, McLaughlin MJ, Kirby JK, Beak D, Chittleborough D. Solubility and batch retention of CeO₂ nanoparticles in soils. *Environ Sci Tech.* 2011; 45:2777–82.
55. Schuurmann G, Ebert RU, Kuhne R. Prediction of the sorption of organic compounds into soil organic matter from molecular structure. *Environ Sci Technol.* 2006; 40:7005–11. [PubMed: 17154008]
56. Puzyn T, Rasulev B, Gajewicz A, Hu XK, Dasari TP, Michalkova A, et al. Using nano-QSAR to predict the cytotoxicity of metal oxide nanoparticles. *Nat Nanotechnol.* 2011; 6:175–8. [PubMed: 21317892]
57. Wootton JT. Predicting direct and indirect effects – an integrated approach using experiments and path-analysis. *Ecology.* 1994; 75:151–165.
58. Wildoer JWG, Venema LC, Rinzler AG, Smalley RE, Dekker C. Electronic structure of atomically resolved carbon nanotubes. *Nature.* 1998; 391:59–62.
59. Guo XY, Wang XL, Zhou XZ, Ding X, Fu B, Tao S, et al. Impact of the simulated diagenesis on sorption of naphthalene and 1-naphthol by soil organic matter and its precursors. *Environ Sci Technol.* 2013; 47:12148–55. [PubMed: 24041398]
60. Wang XL, Xing BS. Roles of acetone-conditioning and lipid in sorption of organic contaminants. *Environ Sci Technol.* 2007; 41:5731–7. [PubMed: 17874780]
61. Chen BL, Chen ZM. Sorption of naphthalene and 1-naphthol by biochars of orange peels with different pyrolytic temperatures. *Chemosphere.* 2009; 76:127–33. [PubMed: 19282020]
62. Masheter AT, Abiman P, Wildgoose GG, Wong E, Xiao L, Rees NV, et al. Investigating the reactive sites and the anomalously large changes in surface pK(a) values of chemically modified carbon nanotubes of different morphologies. *J Mater Chem.* 2007; 17:2616–26.

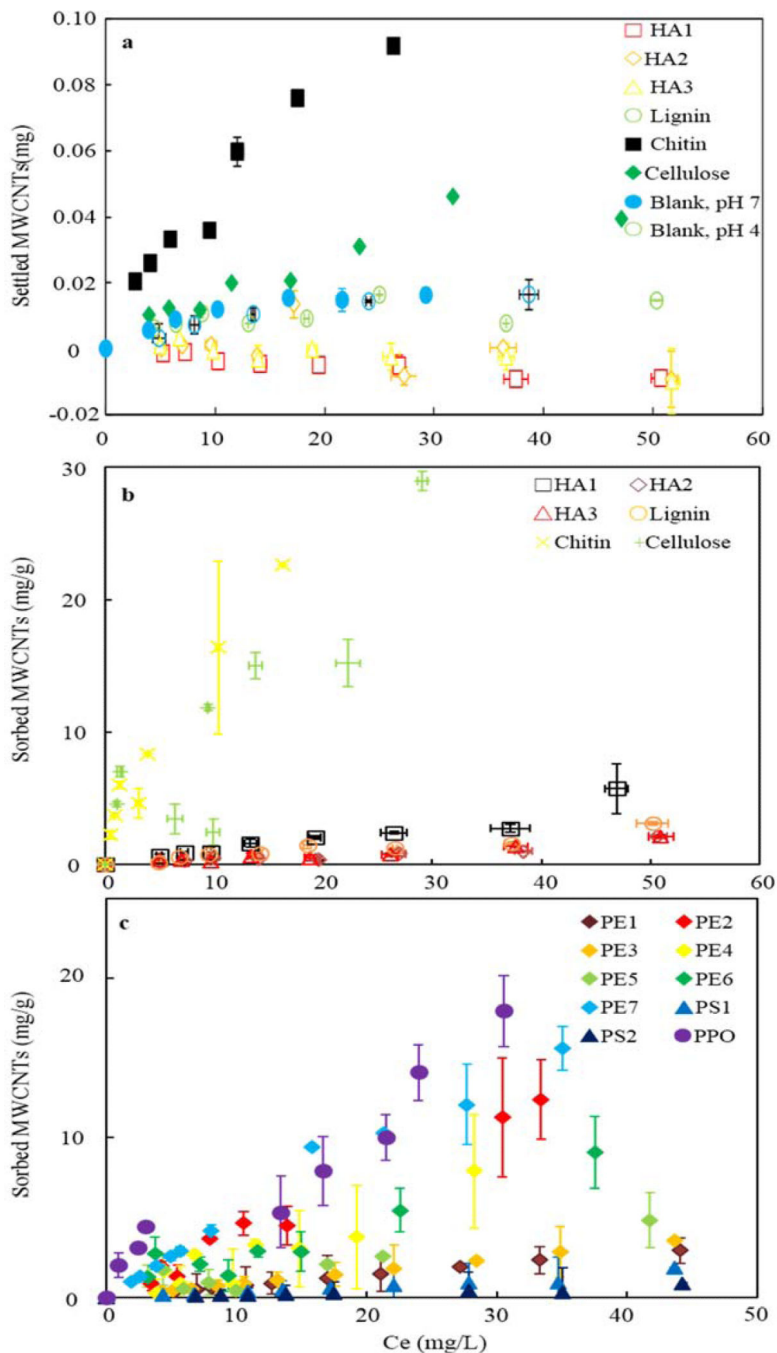


Fig. 1. Phase distribution of MWCNTs. (a) Settling of MWCNTs in different DOM solutions derived from various macromolecules, (b) retention of MWCNTs on natural macromolecules, and (c) retention of MWCNTs on synthetic macromolecules. Error bars represent the standard deviation of three replicates. The amount of settling dramatically decreased in the presence of DOM derived from cellulose, lignin and HAs.

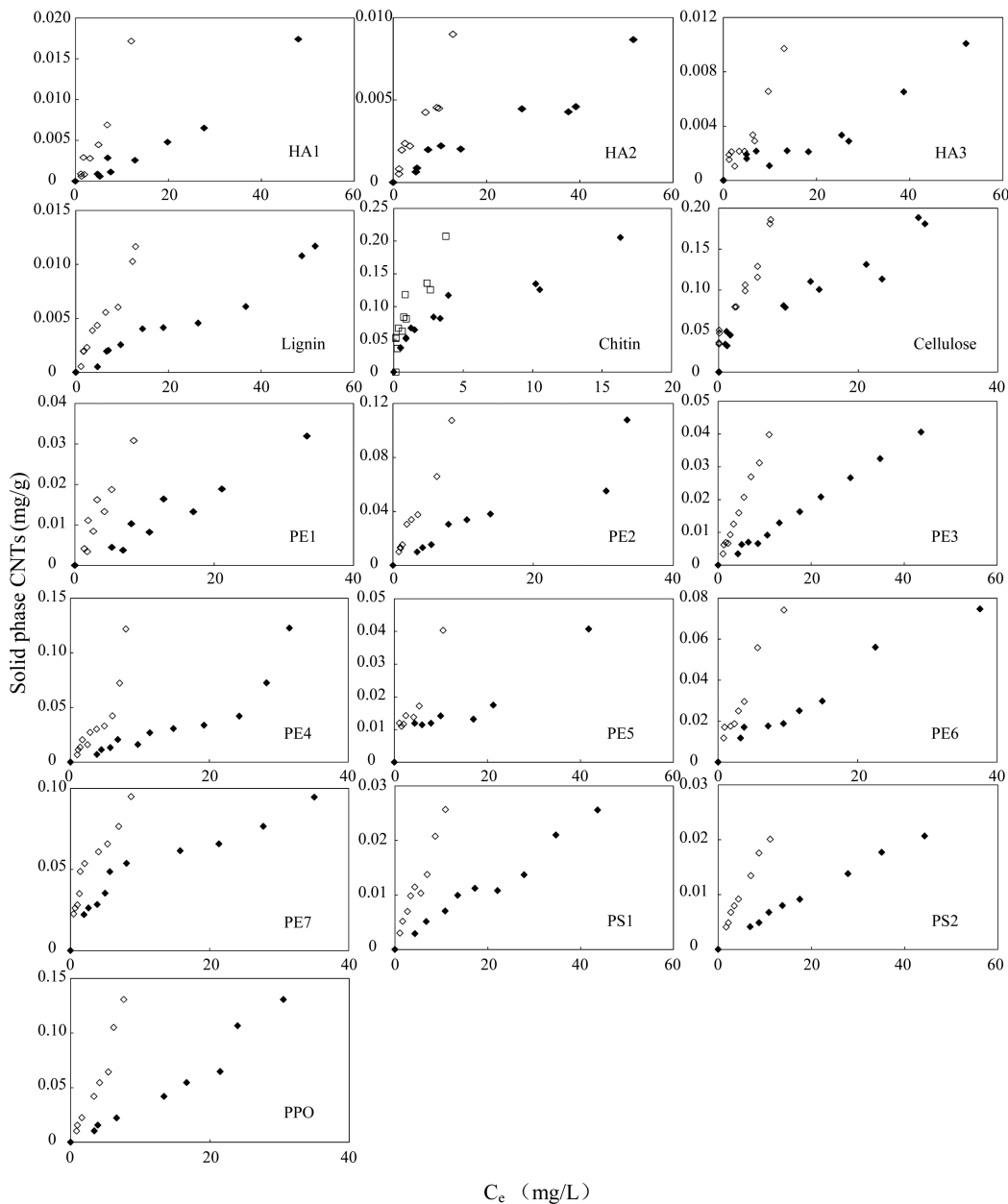


Fig. 2. Redispersion of MWCNTs. Solid phase concentrations before redispersion \blacklozenge and after redispersion \diamond . Error bars represent the standard deviation of three replicates. The amount of MWCNTs in solid phase (including both settled and sorption) remains unchanged after redispersion, suggesting MWCNTs are difficult to re-disperse once they settled down or sorbed onto macromolecules.

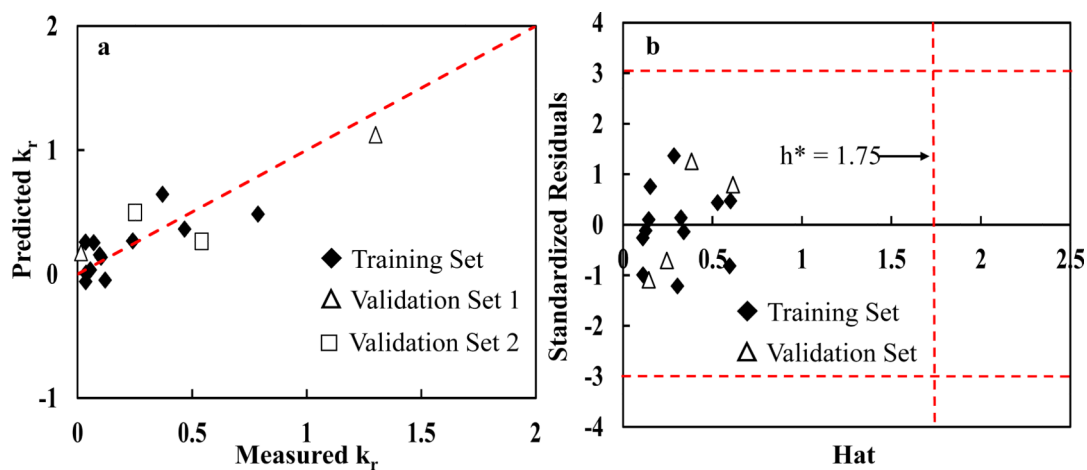


Fig. 3.

(a) Predicted versus measured k_r values of the training and validation macromolecules. Dash line represents 1:1 line. (b) Williams plot for verifying the applicability domain of the model. This figure shows no outliers of training and validation compounds and the predictivity of the model is reliable.

Table 1

Surface and bulk elemental composition of macromolecules.

Sorbent	Surface elemental composition (%)				Bulk elemental composition (%)			
	C	O	N	(O+N)/C	C	O	N	(O+N)/C
HA1	59.1±0.5	22.8±0.2	2.29±0.1	40.6±2.65	48.7±0.2	37.8±0.1	2.8±0.1	83.4±0.6
HA2	74.6±0.2	22.2±0.1	2.88±0.1	33.7±0.35	53.9±0.2	38.3±0.1	2.8±0.1	76.3±0.5
HA3	77.2±2.1	19.5±0.1	3.08±0.1	29.3±0.95	57.6±0.1	32.1±0.1	3.2±0.1	61.3±0.3
Cellulose	62.1±0.1	37.5±0.1	ND	60.4±0.15	41.5±0.1	52.0±0.1	0.1±0.1	125.6±0.3
Lignin	78.3±0.1	20.6±0.3	0.14±0.01	26.5±0.40	62.5±0.3	29.0±0.1	0.7±0.2	47.5±0.7
Chitin	61.6±0.3	30.7±0.4	7.29±0.1	63.9±2.20	43.6±0.1	43.0±0.2	6.3±0.1	113.1±0.7
PE1	98.8±0.3	1.17±0.2	ND	0.01±0.01	85.4±0.1	0.1±0.1	0.2±0.2	ND
PE2	98.5±0.3	1.49±0.1	0.2±0.2	0.02±0.01	85.5±1.0	0.2±0.2	0.0±0.0	ND
PE3	99.5±0.4	0.52±0.1	0.1±0.1	0.01±0.01	85.6±0.3	0.4±0.3	0.1±0.1	ND
PE4	99.2±0.1	0.76±0.01	0.3±0.2	0.01±0.01	85.2±0.2	0.1±0.1	0.2±0.2	ND
PE5	99.4±0.2	0.64±0.1	ND	0.01±0.01	85.7±0.1	ND	0.1±0.1	ND
PE6	96.8±0.3	2.27±0.2	0.9±0.2	0.04±0.01	85.7±0.4	0.2±0.1	0.3±0.2	ND
PE7	98.5±0.1	1.50±0.1	0.2±0.1	0.02±0.01	85.9±0.1	0.3±0.2	0.1±0.1	ND
PS1	97.7±0.2	2.07±0.3	0.1±0.1	0.03±0.01	92.2±0.2	0.1±0.1	0.2±0.1	ND
PS2	97.1±0.1	2.89±0.1	0.3±0.2	0.03±0.01	91.6±0.1	0.2±0.1	0.1±0.1	ND
PPO	89.7±0.1	10.35±0.3	0.2±0.2	11.55±0.55	79.6±0.1	13.7±0.3	ND	17.2±0.4

Error bar represents standard error of three replicates. ND indicates not detected.

Table 2

Selected physicochemical properties of the macromolecules.

Sorbents	Distribution of C chemical shift, ppm (%) ^d						Aromaticity%	Surface Area (m ² g ⁻¹)	DOM (C mg L ⁻¹)	μ^c (cm ² V ⁻¹ s ⁻¹)
	0-50 alkyl	50-108 O-alkyl	108-145 aromatic	145-162 phenolic	162-220 carboxyl					
HA1	16.6±0.1	20.7±0.1	26.2±0.2	12.4±0.1	24.1±0.1	50.9±0.3	1.80±0.03	44.3±0.3	-2.82±0.06	
HA2	17.7±0.1	18.4±0.1	28.8±0.2	12.7±0.1	22.4±0.1	53.5±0.3	1.55±0.01	16.3±0.1	-4.26±0.07	
HA3	22.0±0.1	17.1±0.1	24.1±0.1	10.2±0.1	26.6±0.1	46.7±0.2	3.94±0.04	10.1±0.2	-3.78±0.07	
Cellulose	ND	94.5±0.2	ND	ND	5.5±0.1	0.0±0.0	2.89±0.02	2.10±0.0	-2.17±0.04	
Lignin	13.5±0.0	29.7±0.1	34.0±0.1	15.3±0.0	7.6±0.1	53.3±0.1	3.93±0.06	35.0±0.4	-3.37±0.06	
Chitin	18.3±0.1	60.5±0.2	ND	ND	21.2±0.1	0.0±0.0	14.0±0.1	0.95±0.0	-4.29±0.09	
PE1	100 ^a	0 ^a	0 ^a	0 ^a	0 ^a	0 ^a	6.1±0.06	ND ^b	-2.23±0.06	
PE2	100 ^a	0 ^a	0 ^a	0 ^a	0 ^a	0 ^a	1.4±0.03	ND ^b	-3.56±0.23	
PE3	100 ^a	0 ^a	0 ^a	0 ^a	0 ^a	0 ^a	5.1 ±0.05	ND ^b	-2.29±0.16	
PE4	100 ^a	0 ^a	0 ^a	0 ^a	0 ^a	0 ^a	2.2±0.02	ND ^b	-2.06±0.09	
PE5	100 ^a	0 ^a	0 ^a	0 ^a	0 ^a	0 ^a	10.7±0.08	ND ^b	-2.06±0.10	
PE6	100 ^a	0 ^a	0 ^a	0 ^a	0 ^a	0 ^a	1.6±0.01	ND ^b	-2.45±0.19	
PE7	100 ^a	0 ^a	0 ^a	0 ^a	0 ^a	0 ^a	0.2±0.00	ND ^b	-1.34±0.09	
PS1	25 ^a	0 ^a	75 ^a	0 ^a	0 ^a	75 ^a	0.2±0.00	ND ^b	-2.84±0.10	
PS2	25 ^a	0 ^a	75 ^a	0 ^a	0 ^a	75 ^a	70.2±0.30	ND ^b	-2.08±0.13	
PPO	25 ^a	0 ^a	0 ^a	0 ^a	0 ^a	75 ^a	64.6±0.50	ND ^b	-3.63±0.06	

^aData were calculated according to polymer's formula.^bND indicates not detected.^c μ : Electrophoretic mobility.^dDistribution of C chemical shift (ppm) is percentage of the total signal and the values for each region (i.e., alkyl) are the ratio of the integrated intensity for that region divided by the total integrated intensity. The aromaticity was calculated by expressing the level of aromatic C (108-162 ppm) as the percentage of the total signal. HAs were determined at pH 4 and the rest sorbents were determined at pH 7. Error bar represents standard error of three or more replicates.

Table 3

Observed Pearson correlations between macromolecule properties from MWCNT retention experiments.

	log Surface Polarity	log Aromaticity	log Surface Area	log DOM	log Z
log Surface Polarity	1	0.553	0.178	0.726	0.672
log Aromaticity		1	0.135	0.585	0.169
log Surface Area			1	-0.180	0.854
log DOM				1	-0.312
log Z					1

Table 4

Direct and indirect effect of macromolecule properties on MWCNT retention via path analysis.

Variables	Direct		Indirect			Total
	log Surface Polarity	log Surface Area	log Aromaticity	log Surface Area	log Z	
log Surface Polarity	-0.262	-	0.273	-0.139	-0.111	0.417
log Aromaticity	0.494	-0.145	-	-0.106	-0.090	0.105
log Surface Area	-0.783	-0.047	0.067	-	0.028	0.529
log DOM	-0.153	-0.190	0.289	0.141	-	-0.193
log Z	0.620	-0.176	0.083	-0.669	0.048	-0.094